5-2015

Synthesis of novel dienes and cyclic compounds via olefin metathesis reactions catalyzed by the second generation Grubbs catalyst

Patrick Joseph Carey
University of Tennessee at Chattanooga, zch435@mocs.utc.edu

Synthesis of Novel Dienes and Cyclic Compounds via Olefin Metathesis Reactions Catalyzed by the Second Generation Grubbs Catalyst

Patrick J. Carey

Departmental Honors Thesis
The University of Tennessee at Chattanooga
Department of Chemistry

Project Director: Dr. Kyle S. Knight
Examination Date: March 30, 2015

Members of Examination Committee:
Dr. Titus V. Albu
Dr. Tom R. Rybolt
Dr. D. Stephen Nichols, III

Examining Committee Signatures:

_____
Project Director

_____
Department Examiner

_____
Department Examiner

_____
Liaison, Departmental Honors Committee

_____
Chairperson, University Departmental Honors Committee

Abstract

Transition metal-catalyzed olefin metathesis reactions play a significant role in chemical synthesis. These reactions are currently applied across several disciplines, and their full potential has not yet been reached. This project details the synthesis of spiro[3-cyclopentene-1,9'-[9H]fluorene], 1-(1-amino-2-methylpropyl)-3-cyclopentenol, and the eugenol dimer via olefin metathesis reactions catalyzed by the second generation Grubbs catalyst. The unique structural properties of each compound help demonstrate the widespread abilities of these reactions.

Also reported are the novel three-dimensional crystal structures of both spiro[3-cyclopentene-1,9'-[9H]fluorene] and the eugenol dimer. These structures were determined via X-ray diffraction crystallography methods using a Bruker SMART X2S Single Crystal Diffractometer. Both of these structures have R-values within the accepted publication range of 0.00 – 5.00%

Table of Contents

List of Tables

List of Figures

Introduction

In the modern scientific community, major research efforts are devoted to furthering the field of chemical synthesis. Advances in areas such as biology, material and polymer science, and medicine are all heavily dependent on efficient synthetic procedures, many of which are developed by organic chemists.[1-4] Given the rapid expansion of scientific knowledge over the past few decades, synthetic demands have seemingly reached an all-time high. To contextualize the importance of chemical synthesis within today's highly interdisciplinary world, a 2006 report from the director of the National Institutes of Health (NIH) stated that synthetic organic chemistry was the most substantial obstacle for many biological researchers.[5] In an effort to meet aforementioned demands, many classifications of reactions have been developed. One group of reactions, known as metal-catalyzed olefin metathesis reactions, has made significant contributions to chemical synthesis.[6-11]

Purpose

The primary objective of this project was to synthesize three structurally unique compounds via metal-catalyzed olefin metathesis reactions utilizing the second generation Grubbs catalyst. Specifically, ring-closing metathesis mechanisms were applied to the compounds 9,9-diallylflourene and a terminal diene derivative of L-valine, a common amino acid, and a cross metathesis dimerization mechanism was applied to eugenol. Once these compounds had been synthesized, they were characterized using nuclear magnetic resonance (NMR) techniques and, when applicable, x-ray diffraction crystallography. Ultimately, gaining a more complete understanding of these reactions

and their products will provide more opportunities for future synthetic and crystallographic works.

Olefin metathesis reactions

The underlying principle of transition metal-catalyzed olefin metathesis reactions involves the rearrangement of the carbon atoms around two C=C bonds, known as alkenes or olefins, through the use of an appropriate transition metal-based catalyst. Several advantages to olefin metathesis reactions exist. First and foremost, they enable the synthesis of a very structurally complex product from two simpler compounds.[4] Additionally, these reactions tend to be highly efficient, often producing either no undesirable byproduct or an easily removable byproduct such as ethylene gas.[12] Finally, olefin metathesis reactions are often used to interconvert molecules from one form to another. The pi bonds found within an olefin are reactive enough to be useful in a wide array of transformations yet stable enough to retain structure for extended periods of time.[4]

Olefin metathesis reactions are divided into three major categories: cross metathesis, ring-closing metathesis (RCM), and ring-opening metathesis. These reactions differ from one another in the way the C=C bonds are rearranged.[13] Theoretically, olefin metathesis reactions are reversible. In result, synthetic schemes must be carefully planned to prevent undesired reverse reactions from occurring.[4] Table 1 shows the overview of each of the three forms of olefin metathesis reaction in the presence of an appropriate catalyst.

Table 1: Overview of Olefin Metathesis Reactions	
Reaction	**Overview**
Cross metathesis	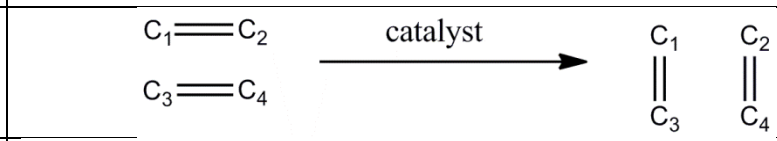
Ring-closing metathesis	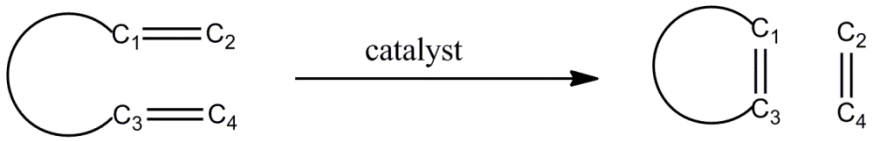
Ring-opening metathesis	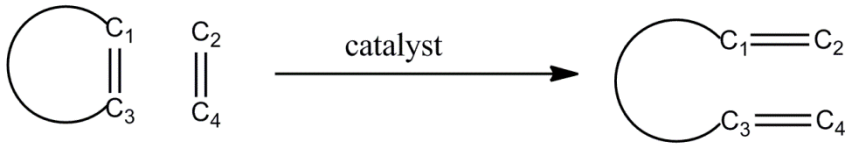

As shown in Table 1, cross metathesis involves the transposition of compounds C_1=C_2 and C_3=C_4 to C_1=C_3 and C_2=C_4.[13] Depending on the structure of each involved olefin, cross metathesis reactions tend to revert back to starting materials more regularly than do ring-closing or ring-opening reactions. Also, in recent years, cross metathesis has proven to be a viable method of dimerization.[14]

Ring-closing metathesis, the most commonly used form of olefin metathesis in industry, involves the reaction of two terminal alkenes in the presence of the catalyst.[15] This process produces a cyclic olefin and another, smaller olefin that can often be easily removed. Removing the smaller product can prevent the reverse reaction from occurring, thus enabling ring-closing reactions to go to completion in the forward direction in some cases.[13, 15]

In ring-opening metathesis, a cyclic olefin reacts with an acyclic olefin to produce an acyclic diene.[16] Due to the release of ring strain, the forward reaction is highly favorable.[17] Ring-opening reactions are very useful in industry, as they can be used to

synthesize several important polymers through a process called ring-opening metathesis polymerization (ROMP).[18-21]

This project focused on the application of ring-closing and cross olefin metathesis reactions. Generalized mechanisms of transition metal-catalyzed ring-closing and cross reactions are given in Figures 1 and 2, respectively. In both mechanisms, the M=Y bond represents the metal carbene that interacts with the olefins of interest. Also, the mechanisms in Figures 1 and 2 were prepared as stepwise representations of the ring-closing and cross metathesis reactions listed in Table 1.

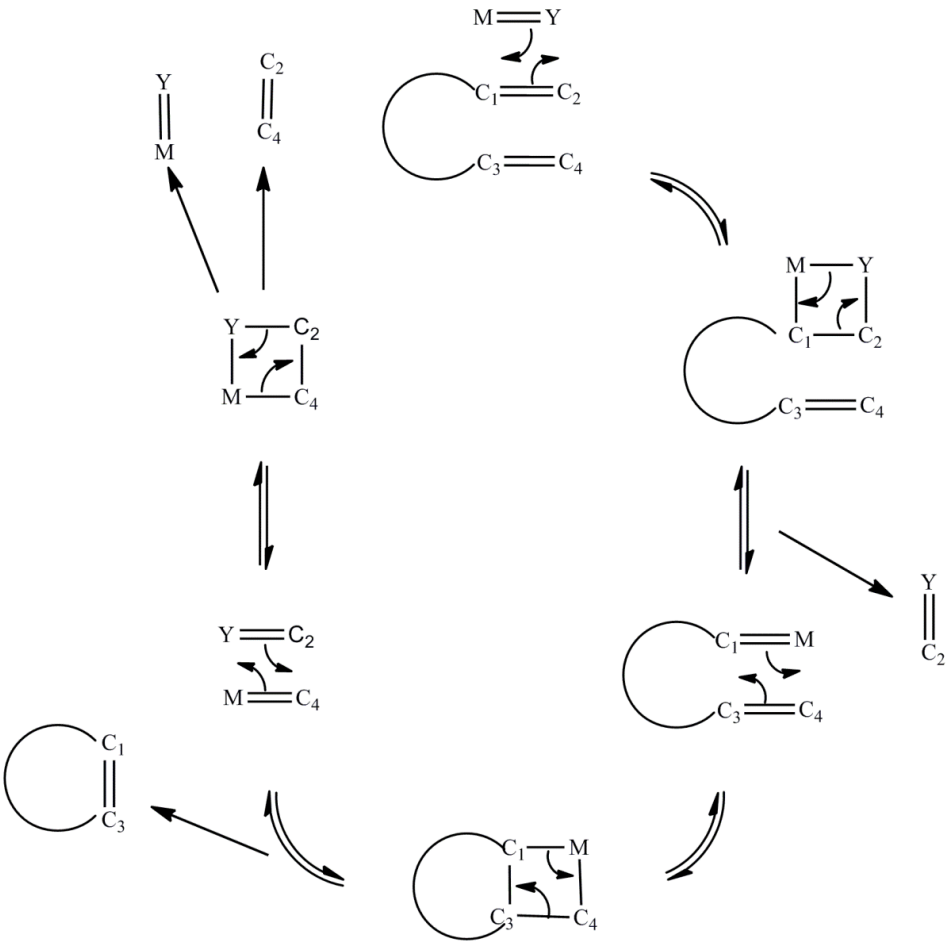

Figure 1: General ring-closing olefin metathesis mechanism[13]

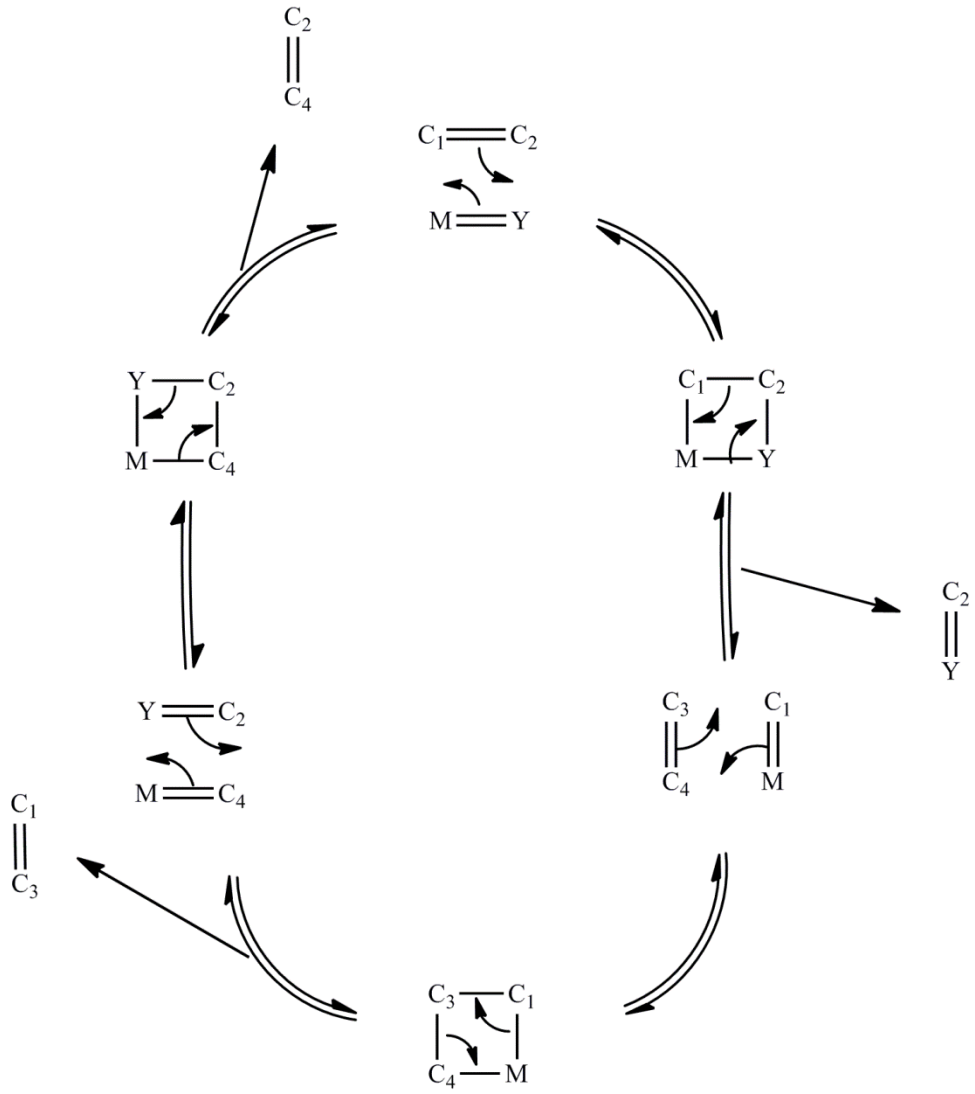

Figure 2: General cross olefin metathesis mechanism[13]

The second generation Grubbs catalyst

Several catalysts have been developed for olefin metathesis reactions. To date, the most effective catalysts have proven to be those containing a ruthenium (atomic symbol Ru) or a molybdenum (atomic symbol Mo) central atom.[4] The central atom plays a significant role in the catalyst's properties. Generally, catalysts containing molybdenum are more active than those containing ruthenium when prepared and

handled under an inert atmosphere.[22-26] Moreover, molybdenum catalysts can remain active in the presence of structurally exposed phosphines or amines, while ruthenium catalysts often cannot.[27] However, ruthenium catalysts are advantageous when working with substrates containing aldehyde, carboxylic acid, or alcohol groups, all of which have displayed the ability to render molybdenum catalysts inactive.[28,29] The second generation Grubbs catalyst was used in this project. The catalyst's structure is shown below in Figure 3.

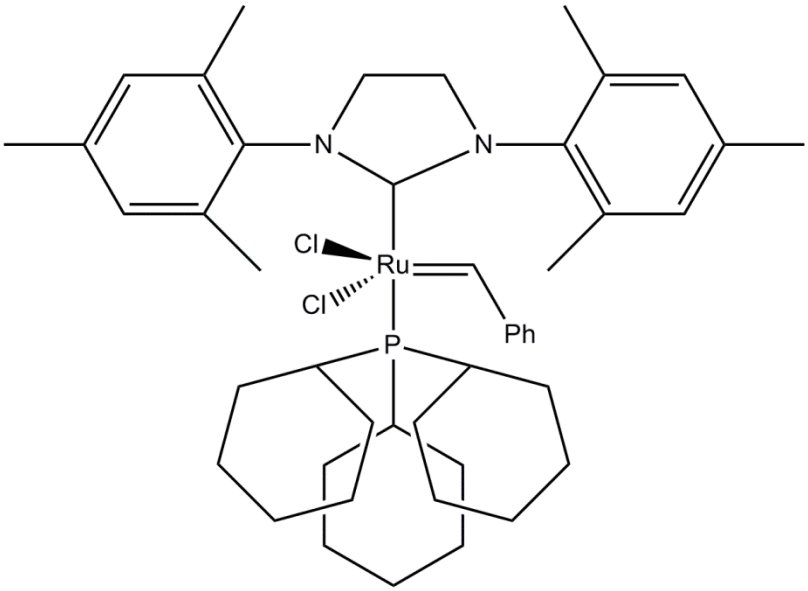

Figure 3: Structure of the second generation Grubbs catalyst

As shown in Figure 3, the second generation Grubbs catalyst is ruthenium-based and achiral. The catalyst's main point of activity with regard to olefin metathesis is the Ru=C bond, commonly called a ruthenium carbene.[30-32] This catalyst has a greater tolerance for water and air than many previous ruthenium- and molybdenum-based catalysts. Additionally, the catalyst has been shown to demonstrate higher ring-closing activity at elevated temperatures with respect to many of its predecessors. Of particular interest is its exceptional catalytic activity at levels as low as 0.05 mol %, making it

among the most cost efficient olefin metathesis catalysts available to an undergraduate research laboratory.[23]

The catalyst was suspended in paraffin wax to preserve its potency. This solid suspension, which will be referred to as the second generation Grubbs catalyst wax dispersion, has been shown to significantly increase the catalyst's shelf life from approximately 30 days to over 18 months.[33] While the paraffin wax does not interfere with the catalyst's reactivity, additional procedures are necessary to isolate the desired reaction product from residual wax.

Substrates used

Previous members of Dr. Knight's research group synthesized a considerable amount of 9,9-diallylfluorene, a yellow liquid. This supply was used to synthesize spiro[3-cyclopentene-1,9'-[9H]fluorene], a four ring system first made via ring-closing metathesis in 1999.[34] However, to date, the synthesis of this compound using the second generation Grubbs catalyst has not been reported, and a solved crystal structure for the compound has not been published.

In recent years, a need for stabilized forms of amino acids has been established. One potential method of increasing stability involves the synthesis of cyclic derivatives of amino acids.[35] In this project, L-valine methyl ester hydrochloride, a salt derivative of the common nonpolar amino acid valine, was used to synthesize a cyclic derivative. The first synthetic step of this process involved creating a valine derivative containing two terminal allyl ($-CH_2-CH=CH_2$) groups. Once this was completed, ring-closing metathesis

procedures using the second generation Grubbs catalyst were performed, thus making 1-(1-amino-2-methylpropyl)-3-cyclopentenol.

Eugenol, a natural product derivative of cinnamon and other spices, has several unique properties that make it a desirable compound for olefin cross metathesis.[36] To date, several cross metathesis reactions of eugenol with other compounds have been reported.[37,38] Despite this, neither a eugenol dimerization via cross metathesis using the second generation Grubbs catalyst nor a solved crystal structure of the eugenol dimer has been published.

X-ray crystallography

X-ray crystallography, a commonly used technique for determining the structure of crystalline compounds, involves exposing a crystalline sample to incident X-ray electromagnetic radiation.[39] Because wavelengths in the X-ray region are approximately the same as the distances between the planes of a crystal, the crystal is able to diffract the incident X-rays. By analyzing the intensities and angles of diffraction, the bond lengths, bond angles, relative atom locations, and atomic vibrations of the molecule of interest can be approximated.[40]

X-ray crystallographic methods are commonly grouped under two classifications: powder diffraction and single crystal diffraction. Single crystal diffraction requires large, homogenous surface area crystals, whereas powder diffraction does not. Generally speaking, powder diffraction data provide far less structural information than do single crystal diffraction data. This is partially due to the random orientation of powder diffraction patterns, which causes the three-dimensional lattice to collapse and appear

one-dimensional. Furthermore, this one-dimensional appearance causes an overlapping of peaks, resulting in increased difficulty when trying to determine individual intensity values. In result, reflection conditions and, ultimately, the determination of a space group are not possible. Both of these are needed to determine a molecular arrangement. In contrast, single crystal diffraction techniques are better able to facilitate the collection of three-dimensional data that can lead to a reliable structural determination.[40]

This project implemented single crystal diffraction techniques to gather structural data. The crystal data were collected using a Bruker SMART X2S Single Crystal X-ray Diffractometer. The computer programs SHELXS97 and SHELXL97 were used to solve and refine crystal structures, respectively.[41] OLEX2 version 1.1 was used as the graphical user interface (GUI) for crystal analysis.[42] This combination of programs can enable the determination and refinement of structures in a fast and efficient manner. The reliability of a structure determined via X-ray diffraction is presented in terms of its R-value, with lower R-values correlating to greater reliability. Generally, publishable structural data have an R-value below 5.00%. Additional viewing studies of the crystal structures were performed using version 3.0.1 of Mercury.[43]

Intermolecular forces

Intermolecular forces are defined as the repulsive or attractive forces which act between neighboring chemical species such as molecules or atoms. Additionally, they generally provide molecular stability in the solid and liquid states of matter and are responsible for many molecular properties, including the ability to crystalize. Noncovalent interactions, those that deal with electrostatic attractions, are responsible for

many of the properties observed in chemical species known to exhibit intermolecular forces.[44]

Biomolecules such as DNA, RNA, proteins, and enzymes are heavily influenced by noncovalent interactions, notably hydrogen bonding and pi stacking.[45] For example, the nitrogenous base pairs of the DNA double helix are held together by hydrogen bonding, a noncovalent interaction in which a hydrogen atom of one molecule interacts electrostatically with a highly electronegative (electron-drawing) atom such as fluorine, oxygen, or nitrogen belonging to an adjacent molecule.[46,47] Pi stacking interactions, interactions dealing with the attractive forces between certain pi electron systems, also play important roles in the chemical properties of several biologically important molecules.[48, 49]

One of the most stable forms of pi stacking is T-shaped stacking. This interaction, also called edge-to-face stacking, involves the placement of a region of positive electrostatic potential (the edge of a ring) in close proximity or contact with an area of negative electrostatic potential (the face of another ring).[50] These interactions often create a "T" shape, and rings that exhibit T-stacking are often perpendicular to one another.[48, 50]

Chromatographic methods

Chromatography is a broad range of methods that are employed to separate a mixture into its individual components. Chromatographic separations are dependent on the movement of a mobile phase through a stationary phase.[51] Three methods of chromatography were employed during this project. Thin layer chromatography (TLC)

was used to track the progress of several reactions. TLC plates used during the project utilized silica gel as the stationary phase and an appropriate solvent as the mobile phase. After placing the plate in a closed chamber containing the solvent, capillary action drew the solvent up the plate. Differences in movement between the starting material and the reaction mixture indicated the formation of a compound with polarity that differed from that of the starting material.[52]

Column chromatography is a common method used to separate the components of non-uniform products.[53] Particularly, this method was used in conjunction with TLC to isolate the desired product of interest from any residual starting materials, side products, catalyst, and paraffin wax. A large glass column with a stopcock was used when multiple impurities needed to be removed. Silica gel served as the stationary phase and was packed into the glass column on top of a layer of glass wool. Multiple solvent mixtures were prepared and were used as mobile phases. These separations were very time consuming and did not always provide sufficient impurity removal, especially for samples over 2 grams. In situations that only required the removal of the catalyst wax dispersion, Pasteur pipet micro-columns were used. These micro-columns were prepared by packing silica gel and glass wool into a small, disposable Pasteur pipet. Normally, only the reaction solvent was used in these separations.

The third chromatographic method used in this project was flash chromatography, an improved form of traditional column chromatography.[54] These separations used the same large glass column as described above. To apply this method, a rubber hose attached to a nitrogen gas line was first fitted through a hole in a rubber septum. The septum was then secured at the top of the glass column. The flow of low-pressure

nitrogen gas through the column significantly improved both separation time and quality, particularly for samples with masses over 2 grams.

Results and Discussion

Synthesis of spiro[3-cyclopentene-1,9'-[9H]fluorene] via RCM

As shown below in Figure 4, spiro[3-cyclopentene-1,9'-[9H]fluorene] (compound **2**, also called dibenzaspirocyclopentane), a yellow crystalline compound, was synthesized from 9,9-diallylfluorene (compound **1**), a yellow liquid, via a ring-closing metathesis reaction catalyzed by the second generation Grubbs catalyst. The reaction follows the general ring-closing mechanism shown in Figure 1. Petroleum ether was chosen as the solvent primarily because it does not coordinate to the catalyst. Substantial bubbling was observed in the reaction vial, signaling the emission of ethylene gas. The percent yields of the recovered product using both 2 mole percent and 5 mole percent catalyst were very similar (46.0 % and 42.3 %, respectively), thus demonstrating the catalyst's potency at low concentrations.

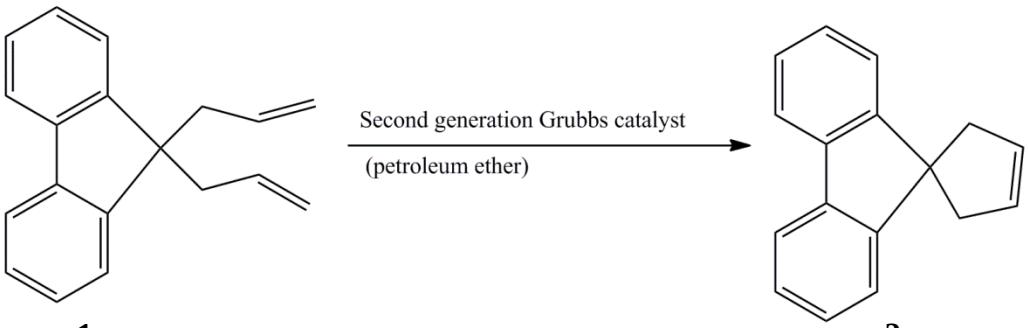

1 **2**

Figure 4: Synthesis of spiro[3-cyclopentene-1,9'-[9H]fluorene]

Figure 5 shows two perspectives of the X-ray crystallographic structure of compound **2**. This structure was obtained via the X-ray diffraction analysis of crystals grown through slow evaporation from petroleum ether. The R-value for this structure was 4.39 %, which falls within the accepted publication range.

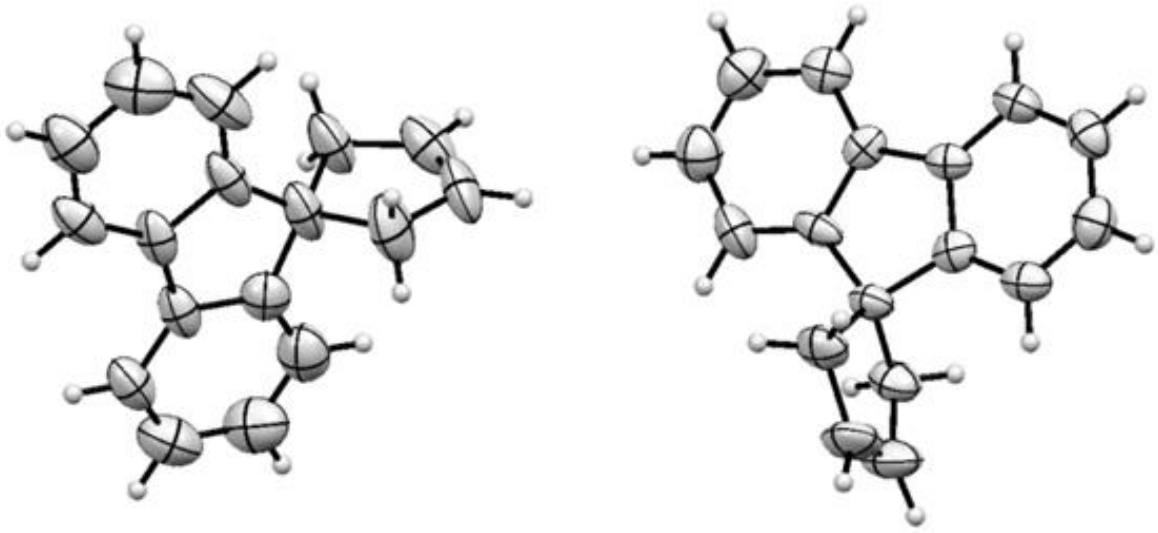

Figure 5: X-ray crystallographic structure of spiro[3-cyclopentene-1,9'-[9H]fluorene]

Preliminary structural analysis shows that three of the compound's rings are in the same plane, while the fourth lies perpendicular to the others, as is demonstrated by a 90° dihedral angle. Figure 6 shows the crystal lattice packing of compound **2**, which suggests the presence of pi stacking. More specifically, the compound demonstrates T-shaped stacking, as is shown in the alignment between the edges and faces of adjacent rings.

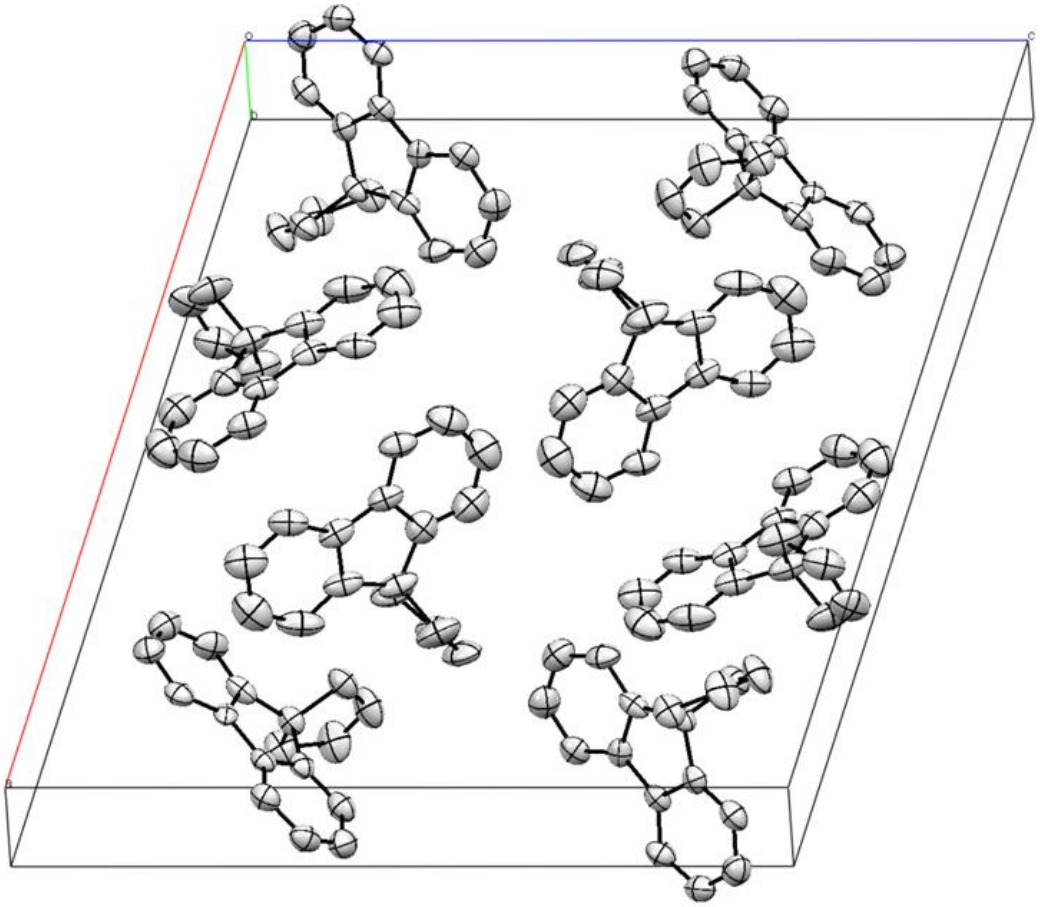

Figure 6: Crystal packing of spiro[3-cyclopentene-1,9'-[9H]fluorene]

A summary of important acquisition and crystallographic data is provided in Table 2, and unit cell parameters are given in Table 3. The complete .cif report for this compound is provided in Appendix I.

Table 2: Acquisition and Crystal Data for Spiro[3-cyclopentene-1,9'-[9H]fluorene]	
Formula	$C_{17}H_{14}$
Molecular Weight	218.28 g/mol
Crystal Density	1.198 g/cm^3
Z	8
Acquisition Temperature	200 K
Volume	2421.0 (10) Å^3
Space Group	P 1 21/c 1
Hall Group	-P 2ybc
R	0.0439
wR^2	0.1426

Table 3: Spiro[3-cyclopentene-1,9'-[9H]fluorene] Unit Cell Parameters		
a = 19.532 (5) Å	b = 6.9894 (17) Å	c = 18.712 (5) Å
α = 90°	β = 106.947 (8) °	γ = 90°

Synthesis of 1-(1-amino-2-methylpropyl)-3-cyclopentenol

The first step in synthesizing the cyclic valine derivative 1-(1-amino-2-methylpropyl)-3-cyclopentenol involved making a terminal diene (compound **4**) from L-valine methyl ester hydrochloride (compound **3**), which is shown in Figure 7. L-valine methyl ester hydrochloride was first dissolved in anhydrous diethyl ether and was then stirred under static nitrogen to facilitate the reaction with allylmagnesium bromide, an air-sensitive Grignard reagent. Upon the addition of allylmagnesium bromide, salt formation was observed. Deionized (DI) water was added to the reaction mixture to quench the excess Grignard reagent. This process caused additional salt formation. A typical aqueous workup using diethyl ether and DI water was performed to separate the

aqueous, salt-containing bottom layer from the top organic layer. Initially, the reaction mixture was very alkaline due to the presence of MgBrOH salt. To make the separation process easier while still maintaining the diene's protonated form, 1 M hydrochloric acid (HCl) was added dropwise to make the mixture slightly alkaline, which was marked by a change from dark blue to faint green on pH paper. After removing the organic solvent, the diene, a yellow liquid, was isolated.

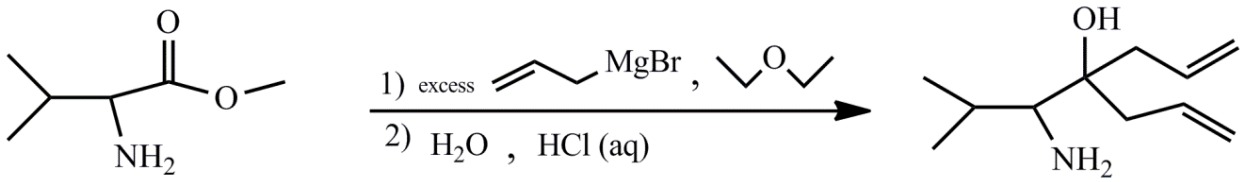

3 HCl **4**

Figure 7: Synthesis of L-valine methyl ester-derived terminal diene

The proposed mechanism of the terminal diene synthesis is shown in Figure 8. The first two steps deal with the addition of allylmagnesium bromide to L-valine methyl ester hydrochloride. The first equivalent of allylmagnesium bromide deprotonates the nitrogen atom. Next, the second equivalent attacks the carbonyl group, resulting in both the delocalization of an electron pair from the carbonyl C=O bond onto the oxygen atom and the formation of a tetrahedral intermediate containing the first allyl group. The carbonyl C=O bond is then reformed, and the CH_3O group acts as a leaving group. An additional Grignard equivalent adds the second allyl group, which also delocalizes a pair of electrons onto the oxygen atom. Due to the inability of the carbonyl carbon's four substituents to act as a leaving group, the tetrahedral structure is maintained. Upon the addition of DI water, both the oxygen atom and amino group are protonated.

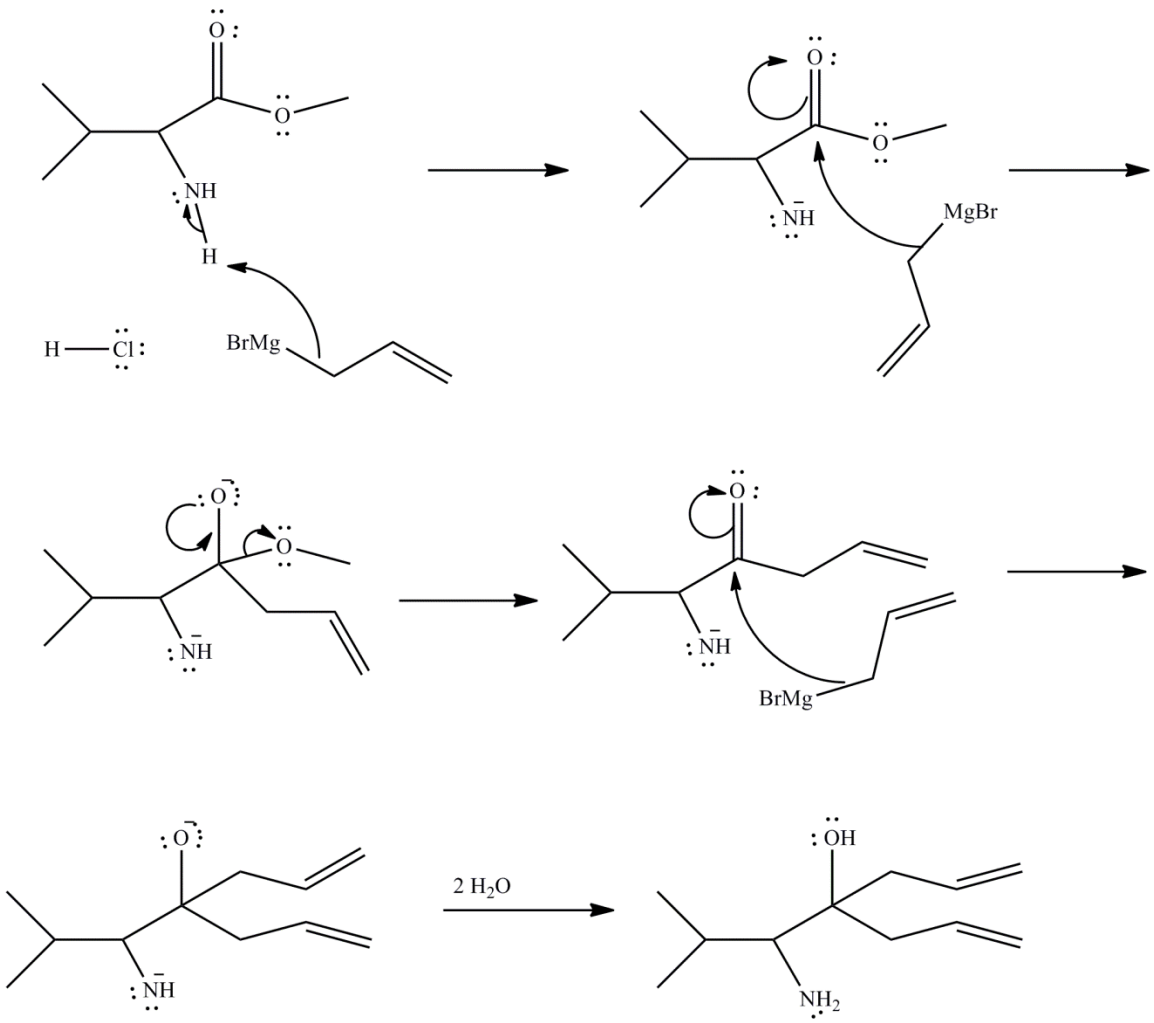

Figure 8: Mechanism of L-valine methyl ester-derived terminal diene synthesis

As shown in Figure 9, 1-(1-amino-2-methylpropyl)-3-cyclopentenol (compound **5**), a white solid, was synthesized via the ring-closing metathesis reaction of the terminal diene **4** catalyzed by the second generation Grubbs catalyst. Dichloromethane was used for this reaction because of its ability to dissolve the terminal diene, which showed significantly reduced solubility in petroleum ether. This reaction follows the general ring-closing metathesis mechanism shown in Figure 1. Traditional column and thin layer chromatography methods were used to isolate the desired product.

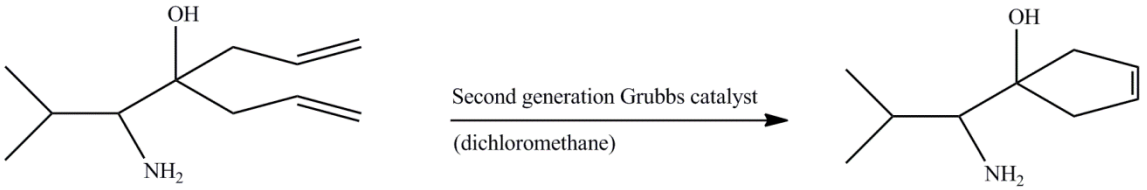

4 **5**

Figure 9: Synthesis of 1-(1-amino-2-methylpropyl)-3-cyclopentenol

Synthesis of eugenol dimer via cross metathesis

Eugenol (compound **6**) was dimerized via a cross metathesis reaction catalyzed by the second generation Grubbs catalyst to form compound **7,** (E)-4,4'-(but-2-ene-1,4-diyl)bis(2-methoxyphenol), as shown in Figure 10. This reaction follows the general cross metathesis mechanism shown in Figure 2 when C_1=C_2 and C_3=C_4 are the same compound. The driving force of the reaction is the emission of ethylene gas. A detailed mechanism for the eugenol dimerization is shown in Figure 11, in which X represents all non-drawn substituents of the second generation Grubbs catalyst, and Ph represents the phenyl group attached to the carbene. Reflux conditions under static nitrogen were utilized to drive the reaction in the forward direction. This reaction was performed on a relatively large scale, which resulted in a substantial amount of paraffin wax from the catalyst dispersion in the final reaction mixture. Flash and thin layer chromatography methods were used to isolate the desired product, a slightly opaque, crystalline solid.

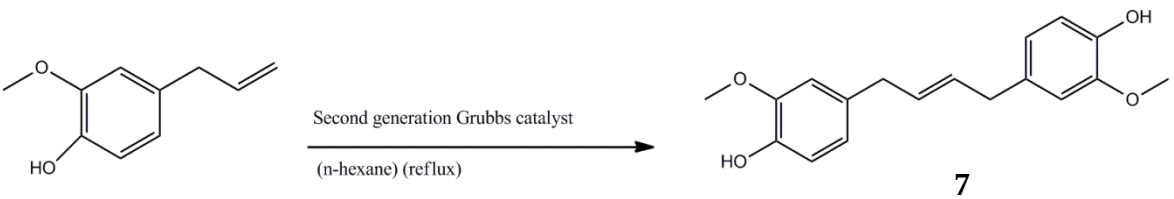

6 **7**

Figure 10: Synthesis of eugenol dimer

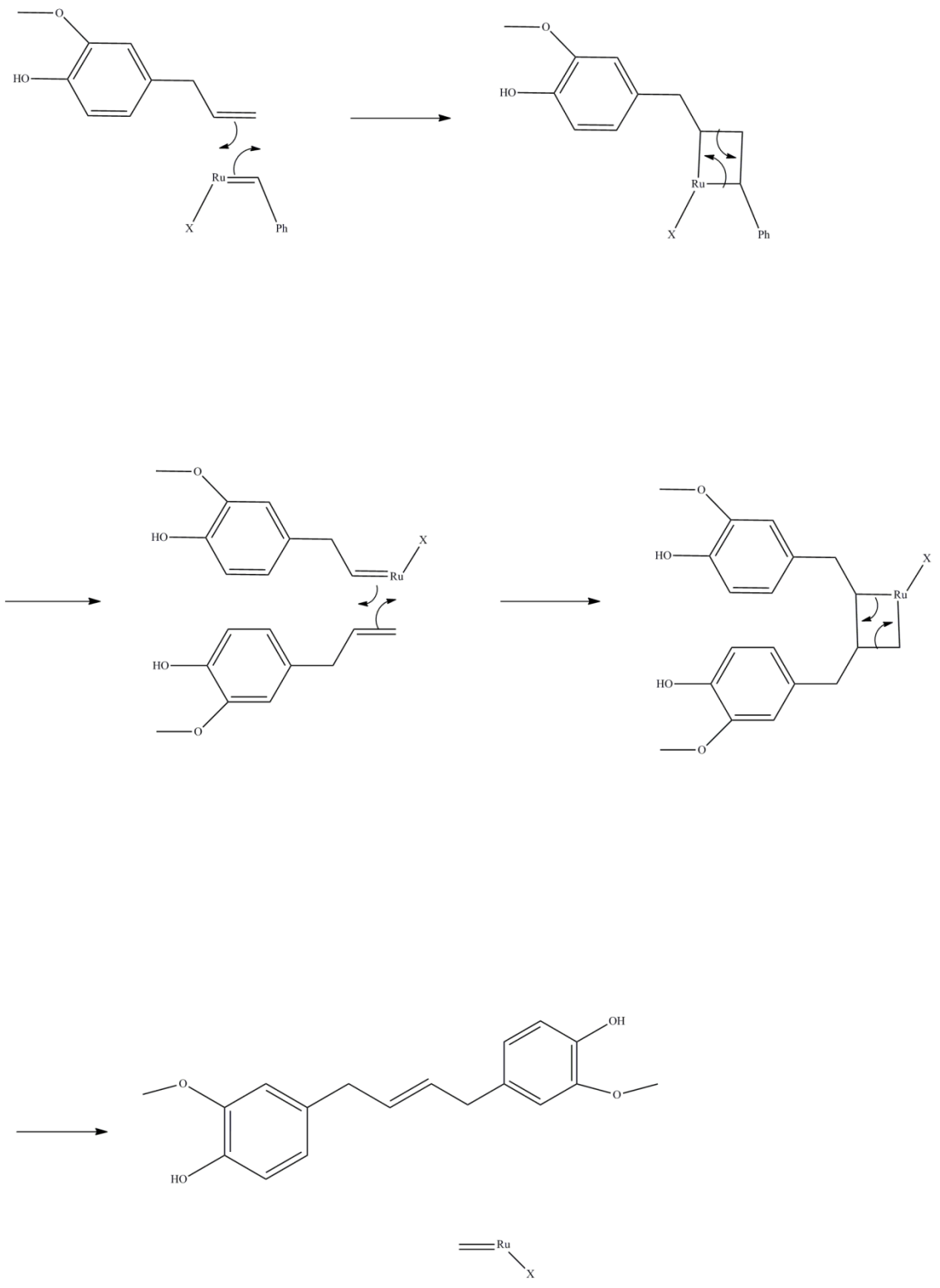

Figure 11: Mechanism of eugenol dimerization

The X-ray crystallographic structure of the eugenol dimer (compound **7**) is shown in Figure 12. This structure was obtained through the X-ray diffraction analysis of crystals grown through slow evaporation from a mixture of n-hexane and ethyl acetate. The structure's R-value is 3.26 %, which falls within the acceptable publication range.

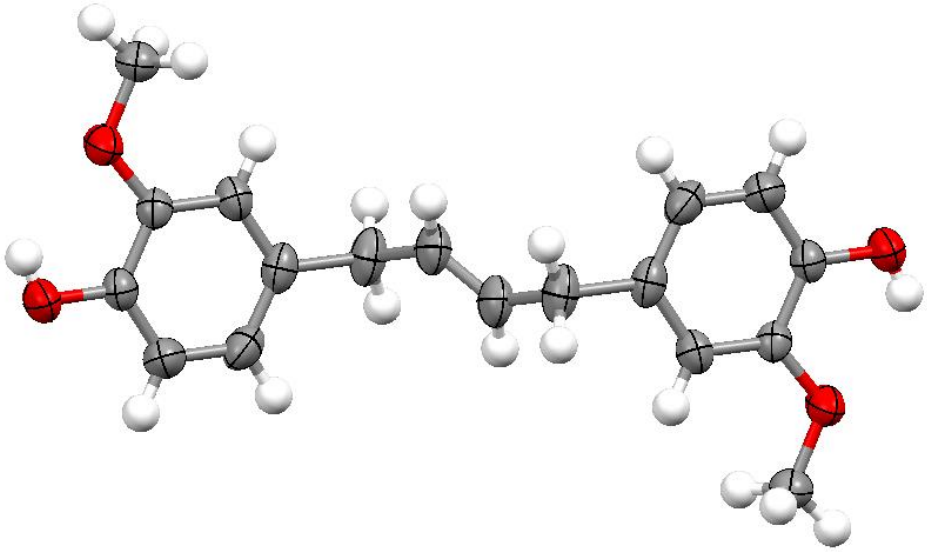

Figure 12: X-ray crystallographic structure of the eugenol dimer

The eugenol dimer's crystal lattice packing, shown in Figure 13, suggests the presence of significant pi stacking. Also, the C=C bond in the chain that links the two rings provides structural rigidity while seemingly maintaining the electronic independence of each ring system.

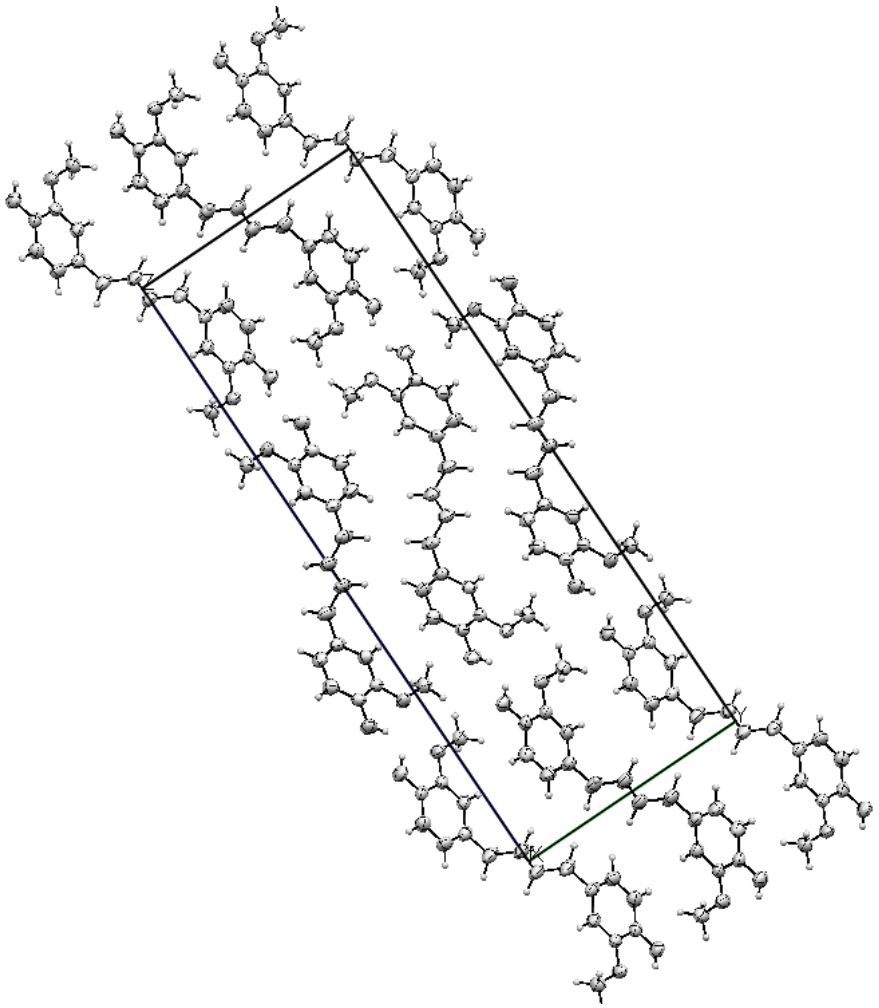

Figure 13: Crystal packing of the eugenol dimer

Preliminary structural analysis suggests the presence of two weak intramolecular hydrogen bonds within the crystal lattice packing. These bonds, shown in Figure 14 and Table 4, have lengths that fall just outside the generally accepted range for this classification of hydrogen bonding.[55] In Table 4, A represents the hydrogen bond donor, and B represents the hydrogen bond acceptor.

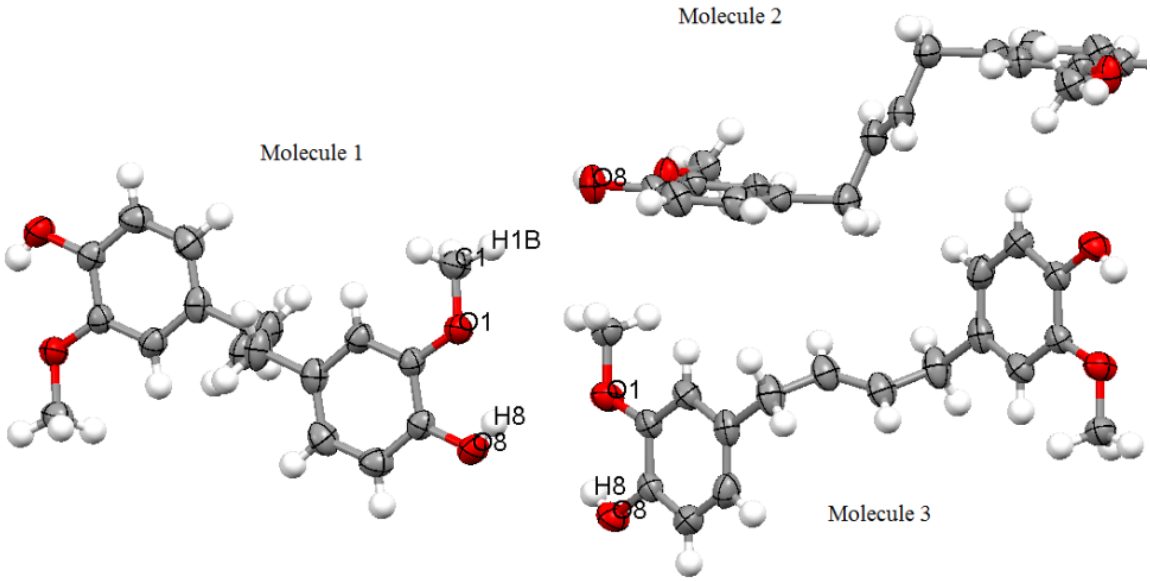

Figure 14: Hydrogen bonding in eugenol dimer lattice

Table 4: Notable hydrogen bond lengths for eugenol dimer		
Bond (A─H---B)	Length (Å)	H-Bond Type
O8(molecule 1)-H8(molecule 1)-O1(molecule 3)	3.341	Weak/Electrostatic
C1(molecule 1)-H1B(molecule 1)-O8(molecule 2)	3.629	Weak/Electrostatic

A summary of important acquisition and crystallographic data is provided in Table 5, and unit cell parameters are given in Table 6.

Table 5: Acquisition and Crystal Data for the Eugenol Dimer	
Formula	$C_{18} H_{20} O_4$
Molecular Weight	300.34 g/mol
Crystal Density	1.291 Mg/m^3
Z	4
Acquisition Temperature	198 K
Volume	1545.33(10) $Å^3$
Space Group	Pbca
R	0.033
wR^2	0.094

Table 6: Eugenol Dimer Unit Cell Parameters		
a = 4.8846(2) Å	b = 10.7002(4) Å	c = 29.5666(11) Å
α = 90°	β = 90°	γ = 90°

Experimental

General comments

All solvents were used as obtained from their respective manufacturers, unmodified in any way. The mass ratio of the second generation Grubbs catalyst wax dispersion used for these reactions was 10 g paraffin wax per 1 g catalyst. All ^1H and ^{13}C experiments performed during this project were carried out using a JEOL 400 MHz FT-NMR, and all NMR data were analyzed using version 4.3.6 of JEOL Delta NMR Software. Crystals were examined using a Meiji Techno polarizing light microscope, and those deemed suitable for X-ray crystallographic analysis were mounted on a Bruker SPINE-Pin using Krytox Vacuum Grease. A Bruker SMART X2S Single Crystal X-ray

Diffractometer was used to collect all crystal structural data, and structural solutions were determined and refined using SHELXS97 and SHELXL97 through the OLEX2 version 1.1. graphical user interface. Version 3.0.1 of Mercury was then used to view the molecular structures.

Spiro[3-cyclopentene-1,9'-[9H]fluorene]

The second generation Grubbs catalyst wax dispersion (707 mg, 2 mol % catalyst) and 9,9-diallylfluorene (1.026 g) were added to a 10 mL screw cap vial containing a spin vane. Petroleum ether was added to bring the reaction mixture volume to 9 mL. The contents were stirred for 36 hours at room temperature while monitored by thin layer chromatography (TLC). After the reaction had run to completion, the mixture components were separated using a Pasteur pipet micro-column. The desired product was collected in a 100 mL beaker and was left for recrystallization via slow evaporation. Once slow evaporation had occurred, the yellow crystals were isolated from residual paraffin wax. The product collected in an optimum yield of 0.418 g (46.0 %). Crystals were then examined under a microscope and were analyzed via x-ray crystallography. The sample was also characterized via ^{1}H NMR. ^{1}H NMR (400 MHz, $CDCl_3$, ppm) δ 7.70 (d, J = 8.2 Hz, 2H), 6.69 (d, J = 6.3 Hz, 2H), 6.67 (s, 2H), 5.63 (m, 2H), 5.45 (s, 2H), 3.85 (s, 6H), 3.29 (d, J = 5.0 Hz, 4H).

1-(1-amino-2-methylpropyl)-3-cyclopentenol

Allylmagnesium bromide (31.20 g, 214.7 mL) and L-valine methyl ester hydrochloride (6.000 g) were added in a 6:1 equivalent ratio to a 250 mL Schlenk flask and were stirred in anhydrous diethyl ether under nitrogen gas. After 10 minutes of

stirring, deionized (DI) H_2O was added to the flask to quench the reaction. The pH was adjusted until slightly alkaline using 1M HCl and pH paper. A standard aqueous workup using deionized water and diethyl ether was performed to separate the aqueous and organic layers. The organic layer was removed via rotary evaporation. The product, a yellow liquid, was collected in an optimum yield of 2.766 g (41.93%) and was characterized via ^1H NMR using D_2O as the solvent. ^1H NMR (400 MHz, D_2O, ppm): δ 5.77 (m, 2H), 5.08 (m, 2H), 5.04 (s, 1H), 4.67 (m, 2H), 2.25 (d, J = 7.3 Hz, 1H), 2.02 (d, J = 4.6 Hz, 4H), 1.58 (m, 1H), 0.89 (d, J = 6.9 Hz, 6H), 0.82 (s, 2H).

The yellow liquid (100 mg) and the second generation Grubbs catalyst wax dispersion (12 mg) were added in a 200:1 equivalent ratio to a 10 mL screw cap vial containing a spin vane. Dichloromethane was added to bring the reaction mixture volume to 9 mL. The vial contents were stirred for 48 hours at room temperature and were monitored by TLC. After stirring had completed, the reaction mixture was separated via flash chromatography on silica gel utilizing varying gradients of n-hexane and ethyl acetate. The product, a white solid, was isolated with a yield of 20.6 mg (24.3%). The product was then characterized via ^1H using $CDCl_3$ as the solvent. ^1H NMR (400 MHz, $CDCl_3$, ppm): δ 5.59 (m, 2H), 5.02 (s, 1H), 2.45 (m, 2H), 2.22 (m, 2H), 2.21 (m, 1H), 1.57 (m, 1H), 0.87 (d, J = 6.4 Hz, 6H), 0.82 (s, 2H).

Eugenol dimer

Eugenol (8.000 g) and the second generation Grubbs catalyst wax dispersion (100 mg) in an equivalent ratio of 100:1 were refluxed in 125 mL of n-hexane under static nitrogen for 48 hours. The reaction mixture components were then separated via

flash chromatography on silica gel utilizing varying gradients of ethyl acetate, n-hexane, and diethyl ether. The fractions were examined using TLC. All fractions were left for slow evaporation, which resulted in the crystal formation. The crystals were isolated with a yield of 2.531 g (34.60%) and were characterized via ^{1}H NMR using $CDCl_3$ as the solvent. Crystals were then examined under a microscope and were analyzed via x-ray crystallography. ^{1}H NMR (400 MHz, $CDCl_3$, ppm): δ 6.83 (d, J = 8.2 Hz, 2H), 6.69 (d, J = 6.3 Hz, 2H), 6.67 (s, 2H), 5.63 (m, 2H), 5.45 (s, 2H), 3.85 (s, 6H), 3.29 (d, J = 5.0 Hz, 4H).

Future Works

The results of this project could lead to additional research endeavors for Dr. Knight's group. First, a complete crystallographic analysis of spiro[3-cyclopentene-1,9'-[9H]fluorene] and the eugenol dimer could be performed. Once this has been completed, the findings could be compared to compounds of similar characteristics as found in the chemical literature. The compounds made in this project could be used for additional synthetic works.

Conclusion

The goal of this project was to synthesize spiro[3-cyclopentene-1,9'-[9H]fluorene], 1-(1-amino-2-methylpropyl)-3-cyclopentenol, and the eugenol dimer via olefin metathesis reactions catalyzed by the second generation Grubbs catalyst. Ultimately, spiro[3-cyclopentene-1,9'-[9H]fluorene] and 1-(1-amino-2-methylpropyl)-3-cyclopentenol were made using ring-closing metathesis reactions, and the eugenol dimer was synthesized via cross metathesis dimerization. Additionally, novel crystal structures

for spiro[3-cyclopentene-1,9'-[9H]fluorene] and the eugenol dimer were reported with R-values of 4.39 % and 3.26 %, respectively. To this point, only basic analysis of these crystal structures has been performed. Gaining a better understanding of the synthesis of these compounds not only contributes to the general knowledge of transition metal-catalyzed olefin metathesis reactions, but it also provides opportunities for future research into reactions involving these types of compounds.

Acknowledgements

Funding for this project was provided by the National Science Foundation, the UTC Department of Chemistry Grote Fund, and the UTC Provost Student Research Award. Additionally, a 5 gram sample of the second generation Grubbs catalyst was generously donated by Materia, Inc.

References

(1) Corey, E.J. The logic of chemical synthesis: Multistep synthesis of complex carbogenic molecules. *Angew. Chem. Int. Edn Engl.*, **1991**, *30*, 455-465.

(2) Meng, D.; Bertinato, P.; Balog, A.; Su, D.; Kamenecka, T.; Sorensen, E.J.; Danishefsky, S.J. Total syntheses of epothilones A and B. *J. Am. Chem. Soc.*, **1997**, *119* (42), 10073-10092.

(3) Rouhi, A.M. Olefin Metathesis: Big Deal Reaction. *Chem. Eng. News*, **2002**, *80*, 29-33.

(4) Hoveyda, A.H.; Zhugralin, A.R. The remarkable metal-catalysed olefin metathesis reaction. *Nature*, **2007**, *450*, 243-251.

(5) Morrissey, S.R. NIH director has steered agency through congressional inquiries and penalty budget increases with bold actions to position agency for future. *Chem. Eng. News*, **2006**, *84* (27), 12-17.

(6) Katz, T.J.; McGinnis, J. The mechanism of the olefin metathesis reaction. *J. Am. Chem. Soc.*, **1975**, *97*, 1592-1593.

(7) Casey, C.P.; Burkhardt, T.J. Reactions of (diphenylcarbene)pentacarbonyltungsten(0) with alkenes. Role of metal-carbene complexes in cyclopropanation and olefin metathesis reactions. *J. Am. Chem. Soc.*, **1974**, *96*, 7808-7809.

(8) Grubbs, R.H.; Carr, D.D.; Hoppin, C.; Burk, P.L. Consideration of the mechanism of the metal catalyzed olefin metathesis reaction. *J. Am. Chem. Soc.*, **1976**, *98*, 3478-3483.

(9) Schrock, R.R. Multiple metal-carbon bonds for catalytic metathesis reactions. *Angew. Chem. Int. Edn.*, **2006**, *45*, 3748-3759.

(10) Grubbs, R.H. Olefin metathesis molecules for the preparation of molecules and materials. *Angew. Chem. Int. Edn.*, **2006**, *45*, 3760-3765.

(11) Chauvin, Y. Olefin metathesis: The early days. *Angew. Chem. Int. Edn.*, **2006**, *45*, 3740-3747.

(12) Trost, B.M. The atom economy – a search for synthetic efficiency. *Science*, **1991**, *254*, 1471-1478.

(13) *Handbook of Metathesis*; Grubs, R.H., Ed.; Wiley-VCH: Weinheim, Germany, 2003.

(14) De la Torre, M.C.; Deometrio, A.; Alvaro, E.; Garcia, I.; Sierra, M.A. Synthesis of α-onoceradiene-like terpene dimers by intermolecular metathesis processes. *Org. Lett.*, **2006**, *8*, 593-596.

(15) Han,S.; Chang, S. General Ring-Closing Metathesis. In *Handbook of Metathesis*; Grubbs, R.H., Ed.; Wiley-VCH: Weinheim, Germany, 2003; Vol. 2, pp 5-127.

(16) Schrader, T. O.; Snapper, M.L. Ring-Opening Cross Metatheses. In *Handbook of Metathesis*; Grubbs, R.H., Ed.; Wiley-VCH: Weinheim, Germany, 2003; Vol. 2, pp 205-237.

(17) Wiberg, K.B. The concept of strain in organic chemistry. *Angew. Chem. Int. Edn Engl.*, **1986**, *25*, 312-322.
(18) Mol, J.C. Industrial applications of olefin metathesis. *J. Mol. Catal. A.*, **2004**, *213*, 39-45.
(19) Khosravi, E. Synthesis of Copolymers. In *Handbook of Metathesis*; Grubbs, R.H., Ed.; Wiley-VCH: Weinheim, Germany, 2003; Vol. 3, pp 72-117.
(20) Feast, W.J. Conjugated Polymers. In *Handbook of Metathesis*; Grubbs, R.H., Ed.; Wiley-VCH: Weinheim, Germany, 2003; Vol. 3, pp 118-142.
(21) Hamilton, J.G. Stereochemistry of Ring-Opening Metathesis Polymerization. In *Handbook of Metathesis*; Grubbs, R.H., Ed.; Wiley-VCH: Weinheim, Germany, 2003; Vol. 3, pp 143-179.
(22) Schrock, R.R.; Murdzek, J.S.; Bazan, G.C.; Robbins, J.; DiMare, M.; O'Regan, M. Synthesis of molybdenum imido alkylidene complexes and some reactions involving acyclic olefins. *J. Am. Chem. Soc.*, **1990**, *112*, 3875-3886.
(23) Scholl, M.; Ding, S.; Lee, C.W.; Grubbs, R. H. Synthesis and activity of a new generation of ruthenium-based olefin metathesis catalysts coordinated with 1,3-dimesityl-4,5-dihydroimidazol-2-ylidene ligands. *Org. Lett.*, **1999**, *1*, 953-956.
(24) Weskamp, T.; Schattenmann, W.C.; Spegler, M.; Herrmann, W.A. A novel class of ruthenium catalysts for olefin metathesis. *Angew. Chem. Int. End Engl.*, **1995**, *37*, 2490-2493.
(25) Huang, J.; Stevens, E.D.; Nolan, S.P.; Petersen, J.L. Olefin metathesis – active ruthenium complexes bearing nucleophilic carbene ligand. *J. Am. Chem. Soc.*, **1999**, *121*, 2674-2678.
(26) Garber, S.B.; Kingsbury, J.S.; Gray, B.L.; Hoyveda, A.H. Efficient and recyclable monomeric and dendritic Ru-based metathesis catalysts. *J. Am. Chem. Soc.*, **2000**, *122*, 8168-8179.
(27) Schrock, R.R.; Hoyveda, A.H. Molybdenum and tungsten imido alkylidene complexes as efficient olefin metathesis catalysts. *Angew. Chem. Int. Edn*, **2003**, *42*, 4592-4633.
(28) Cortez, G.A.; Schrock, R.R.; Hoyveda, A.H. Efficient enantioselective synthesis of piperidines through catalytic asymmetric ring-opening/cross-metathesis reactions. *Agnew. Chem. Int. End*, **2007**, *46*, 4534-4538.
(29) Slinn, C.A.; Redgrave, A.J.; Hind, S.L.; Edlin, C.; Nolan, S.P.; Gouverneur, V. Synthesis of unprotected and borane-protected phosphines using Ru- and Mo-based olefin metathesis catalysts. *Org. Biomolec. Chem.*, **2003**, *1*, 3820-3825.
(30) Nguyen, S.B.T.; Trnka, T.M. The Discovery and Development of Well-Defined, Ruthenium-Based Olefin Metathesis Catalysts. In *Handbook of Metathesis*; Grubbs, R.H., Ed.; Wiley-VCH: Weinheim, Germany, 2003; Vol. 1, pp 61-85.

(31) Roper, W.R. Synthesis of Ruthenium Carbene Complexes. In *Handbook of Metathesis*; Grubbs, R.H., Ed.; Wiley-VCH: Weinheim, Germany, 2003; Vol. 1, pp 86-94.
(32) Sanford, M.S.; Love, J.A. Mechanism of Ruthenium-Catalyzed Olefin Metathesis Reactions. In *Handbook of Metathesis*; Grubbs, R.H., Ed.; Wiley-VCH: Weinheim, Germany, 2003; Vol. 1, pp 112-131.
(33) Taber, D.F.; Frankowski, K.J. Grubbs' catalyst in paraffin: An air-stable preparation for alkene metathesis. *JOC Note*, **2000**, *68*, 6047-6048.
(34) Kotha, S.; Manivannan, E.; Sreenivasachary, N.; Deb, A. Spiro-annulation via ring closing metathesis reaction. *Synlett*, **1999**, *10*, 1618-1620.
(35) Deber, C.M.; Blout, E.R. Cyclic peptides. Amino acid-cyclic peptides. *J. Am. Chem. Soc.*, **1974**, *96*, 7566-7568.
(36) Mallavarapu, G.R.; Ramesh, S.; Chandrasekhara, R.S.; Rajeskwara Rao, B.R.; Kaul, P.N.; Bhattacharya, A.K. Investigation of the essential oil of cinnamon leaf grown at Bangalore and Hyderabad. *Flavour Fragr. J.*, **1995**, *10*, 239-242.
(37) Taber, D.F.; Frankowski, K.J. Grubbs's cross metathesis of eugenol with cis-2-butene-1,4-diol to make a natural product. An organometallic experiment for the undergraduate lab. *J. Chem. Educ.*, **2006**, *83*, 283-284.
(38) Blackwell, H.E.; O'Leary, D.J.; Chatterjee, A.K.; Washenfelder, R.A.; Bussman, D.A.; Grubbs, R.H. New approaches to olefin cross-metathesis. *J. Am. Chem. Soc.*, **2000**, *122*, 58-71.
(39) Palenik, G.J.; Jensen, W.P.; Suh, I. The history of molecular structure determination viewed through the Nobel Prizes. *J. Chem. Educ.*, **2003**, *80*, 753-761.
(40) Lapidus, S.H.; Stephens, P.W.; Arora, K.K.; Shattock, T.R.; Zaworotko. A comparison of cocrystal structure solutions from powder and single crystal techniques. *Cryst. Growth Des.*, **2010**, *10*, 4630-4637.
(41) Sheldrick, G.M. *Acta Cryst.*, **2008**, *A64*, 112-122.
(42) Dolomonov, O.V.; Bourhis, L.J.; Gildea, R.J.; Howard, J.A.K.; Puschmann, H. *J. App;. Cryst.*, **2009**, *42*, 339-341.
(43) Macrae, C.F.; Bruno, I.J.; Chisholm, J.A.; Edgington, P.R.; McCabe, P.; Pidcock, E.; Rodriquez-Monge, L.; Taylor, R.; van de Streek, J.; Wood, P.A. *J. Appl. Cryst.*, **2008**, *41*, 466.
(44) Burdge, J.; Overby, J. *Chemistry: Atoms First*, 1st ed.; McGraw-Hill: New York, 2012; pp 464-498.
(45) Saenger, W. *Principles of Nucleic Acid Structure*; Springer-Verlag: New York, 1984.
(46) Watson, J.D.; Crick, F.H.C. A structure for deoxyribose nucleic acid. *Nature*, **1953**, *171*, 737-738.

(47) Shieh, H.S.; Berman, H. M.; Dabrow, M.; Neidle, S. The structure of drug-deoxydinucleoside phosphate complex; generalized conformational behavior of intercalation complexes with RNA and DNA fragments. *Nucleic Acids Res*., **1980**, *8*, 85–97.

(48) Burley, S. K.; Petsko, G. A. Aromatic-aromatic interaction: a mechanism of protein structure stabilization. *Science*, **1985**, *229*, 23– 28.

(49) Meyer, E. A.; Castellano, R. K.; Diederich, F. Interactions with aromatic rings in chemical and biological recognition *Angew. Chem. Int. Ed. Engl.* **2003**, *42*, 1210–1250.

(50) Anslyn, E.V.; Dougherty, D.A. *Modern Physical Organic Chemistry*; University Science Books: Sausalito, California, 2006; pp 180-188.

(51) Novák, J.; Janák, J. Theoretical Aspects of Liquid Chromatography. In *Liquid Column Chromatography: A Survey of Modern Techniques and Applications*; Deyl, Z., Macek, K., Janák, J., Eds.; Elsevier Scientific Publishing Company: Amsterdam, 1975; pp 3-10.

(52) Touchstone, J.C. *Practice of Thin Layer Chromatography*, 3rd ed.; John Wiley & Sons, Inc.: Hoboken, New Jersey, 1992; pp 1-68.

(53) Novák, J.; Janák, J.; Wičar, S. Basic Processes of the Chromatographic Process. In *Liquid Column Chromatography: A Survey of Modern Techniques and Applications*; Deyl, Z., Macek, K., Janák, J., Eds.; Elsevier Scientific Publishing Company: Amsterdam, 1975; pp 11-24.

(54) Still, W.C.; Kahn, M.; Mitra, A. Rapid chromatographic technique for preparative separations with moderate resolution. *J. Org. Chem.*, **1978**, *43*, 2923-2925.

(55) Jeffrey, G. *An Introduction to Hydrogen Bonding*; 1st ed.; Oxford University Press: New York, New York, 1997; pp 12-14.

Appendix I

Spiro[3-cyclopentene-1,9'-[9H]fluorene] Report

Table 1. Crystal data and structure refinement for dibenzaspirocyclopentane.

Identification code	dibenzaspirocyclopentane
Empirical formula	$C_{17}H_{14}$
Formula weight	218.28
Temperature	200(2) K
Wavelength	0.71073 Å
Crystal system	Monoclinic
Space group	P 1 21/c 1
Unit cell dimensions	a = 19.352(5) Å b = 6.9894(17) Å c = 18.712(5) Å α = 90° β = 106.947(8)° γ = 90°
Volume	2421.1(10) $Å^3$
Z	8
Density (calculated)	1.198 Mg/cm^3
Absorption coefficient	0.067 mm^{-1}
F(000)	928
Crystal size	0.05 x 0.35 x 0.44 mm^3
Theta range for data collection	1.10 to 17.66°
Index ranges	-16<=h<=15, -5<=k<=5, -15<=l<=15
Reflections collected	11618
Independent reflections	1561 [R(int) = 0.0607]
Completeness to theta = 17.66°	99.6%
Absorption correction	Multiscan
Max. and min. transmission	0.9966 and 0.8161
Refinement method	Full-matrix least-squares on F^2
Data / restraints / parameters	1561 / 0 / 308
Goodness-of-fit on F^2	1.109

Final R indices [I>2sigma(I)]	R1 = 0.0447, wR2 = 0.1088
R indices (all data)	R1 = 0.0716, wR2 = 0.1503
Extinction coefficient	0.014(2)
Largest diff. peak and hole	0.207 and -0.222

Table 2. Atomic coordinates ($x10^4$) and equivalent isotropic displacement parameters ($Å^2x10^3$) for dibenzaspirocyclopentane.

U(eq) is defined as one third of the trace of the orthogonalized U^{ij} tensor.

Atom	x	y	z	U(eq)
C1	8448(3)	4599(9)	4133(3)	72(2)
C2	8326(3)	2684(7)	3784(3)	55(2)
C3	8829(3)	2653(7)	3275(3)	41(1)
C4	8533(4)	1541(8)	2555(4)	42(2)
C5	7910(4)	1813(8)	1971(5)	57(2)
C6	7768(3)	629(10)	1351(4)	62(2)
C7	8242(4)	-801(9)	1306(4)	59(2)
C8	10668(4)	822(10)	4514(3)	57(2)
C9	10055(5)	1960(7)	4297(4)	50(2)
C10	9537(3)	1595(8)	3637(4)	40(2)
C11	8960(3)	4811(7)	3159(3)	56(2)
C12	8785(3)	5740(8)	3789(3)	71(2)
C13	8862(4)	-1097(7)	1884(4)	47(2)
C14	9014(3)	63(8)	2514(4)	35(1)
C15	9627(4)	89(8)	3182(4)	37(1)
C16	10246(4)	-1064(7)	3405(4)	46(2)
C17	10757(3)	-686(9)	4068(5)	51(2)
C18	6667(4)	3263(9)	-592(4)	73(2)
C19	6239(3)	4157(7)	-1290(4)	73(2)
C20	6375(3)	6375(7)	-1153(4)	59(2)
C21	5713(3)	7368(9)	-1048(4)	56(2)
C22	5361(5)	6988(8)	-533(4)	73(2)
C23	4745(5)	8018(12)	-552(4)	85(2)

Atom	x	y	z	U(eq)
C24	4498(4)	9445(10)	-1081(5)	79(2)
C25	6931(4)	8262(12)	-2834(5)	84(2)
C26	6410(5)	9626(10)	-3064(4)	76(2)
C27	5921(3)	9917(8)	-2668(5)	58(2)
C28	5946(4)	8830(9)	-2054(4)	49(2)
C29	6474(4)	7415(9)	-1817(4)	55(2)
C30	6973(3)	7134(8)	-2212(5)	78(2)
C31	7028(3)	6465(9)	-439(4)	82(2)
C32	7091(3)	4480(11)	-136(4)	74(2)
C33	5472(4)	8806(9)	-1575(4)	49(2)
C34	4864(4)	9854(7)	-1593(4)	60(2)

Table 3. Bond lengths (Å) and angles (°) for dibenzaspirocyclopentane.

C1-C12	1.312(6)
C1-C2	1.478(7)
C2-C3	1.549(6)
C3-C4	1.515(7)
C3-C10	1.530(7)
C3-C11	1.555(6)
C4-C5	1.384(7)
C4-C14	1.407(6)
C5-C6	1.386(7)
C6-C7	1.376(7)
C7-C13	1.378(7)
C8-C17	1.386(7)
C8-C9	1.387(7)
C9-C10	1.369(7)
C10-C15	1.395(6)
C11-C12	1.469(6)
C13-C14	1.390(7)
C14-C15	1.450(7)
C15-C16	1.403(7)
C16-C17	1.368(6)

C18-C32	1.310(7)
C18-C19	1.467(7)
C19-C20	1.580(7)
C20-C21	1.519(8)
C20-C29	1.499(7)
C20-C31	1.550(7)
C21-C33	1.390(7)
C21-C22	1.358(7)
C22-C23	1.384(8)
C23-C24	1.388(8)
C24-C34	1.377(7)
C25-C26	1.364(8)
C25-C30	1.388(8)
C26-C27	1.375(7)
C27-C28	1.367(7)
C28-C29	1.398(7)
C28-C33	1.456(7)
C29-C30	1.391(8)
C31-C32	1.490(8)
C33-C34	1.379(7)

C12-C1-C2	111.9(5)
C1-C2-C3	103.7(4)
C4-C3-C10	101.7(4)
C4-C3-C2	114.3(4)
C10-C3-C2	112.1(4)
C4-C3-C11	114.2(4)
C10-C3-C11	111.6(4)
C2-C3-C11	103.3(4)
C5-C4-C14	119.7(5)
C5-C4-C3	130.4(6)
C14-C4-C3	109.9(6)
C4-C5-C6	119.6(5)
C5-C6-C7	120.8(6)
C13-C7-C6	120.3(5)
C17-C8-C9	120.4(5)
C10-C9-C8	119.8(5)
C15-C10-C9	120.1(5)

C15-C10-C3	110.4(6)
C9-C10-C3	129.4(6)
C12-C11-C3	103.5(4)
C1-C12-C11	112.9(5)
C7-C13-C14	119.9(5)
C13-C14-C4	119.7(6)
C13-C14-C15	131.0(6)
C4-C14-C15	109.4(6)
C10-C15-C16	120.0(6)
C10-C15-C14	108.6(6)
C16-C15-C14	131.5(6)
C17-C16-C15	119.2(5)
C16-C17-C8	120.6(5)
C32-C18-C19	112.7(6)
C18-C19-C20	104.4(5)
C21-C20-C29	101.7(5)
C21-C20-C31	112.1(5)
C29-C20-C31	115.2(5)
C21-C20-C19	111.3(5)
C29-C20-C19	113.3(5)
C31-C20-C19	103.6(4)
C33-C21-C22	120.7(6)
C33-C21-C20	111.1(6)
C22-C21-C20	128.2(7)
C21-C22-C23	119.1(6)
C24-C23-C22	120.5(6)
C23-C24-C34	120.3(5)
C26-C25-C30	121.2(6)
C25-C26-C27	119.7(6)
C28-C27-C26	120.7(6)
C27-C28-C29	120.2(6)
C27-C28-C33	130.5(7)
C29-C28-C33	109.3(6)
C28-C29-C30	119.2(6)
C28-C29-C20	110.3(6)
C30-C29-C20	130.5(7)
C29-C30-C25	119.1(6)
C32-C31-C20	104.2(5)

C18-C32-C31	113.0(6)
C21-C33-C34	120.6(6)
C21-C33-C28	107.7(6)
C34-C33-C28	131.7(7)
C33-C34-C24	118.8(5)

Table 4. Anisotropic displacement parameters ($Å^2x10^3$) for dibenzaspirocyclopentane.

The anisotropic displacement factor exponent takes the form: $-2\pi^2[h^2 a^{*2} U^{11} + ... + 2 h k a^* b^* U^{12}]$

	U^{11}	U^{22}	U^{33}	U^{23}	U^{13}	U^{12}
C1	98(5)	58(4)	79(5)	-8(4)	-8(4)	12(4)
C2	55(4)	52(4)	68(4)	1(3)	1(3)	9(3)
C3	49(4)	30(4)	50(4)	-1(3)	-1(3)	5(3)
C4	46(5)	24(4)	67(6)	5(4)	5(4)	4(4)
C5	44(5)	52(4)	70(5)	18(4)	18(4)	12(3)
C6	59(5)	60(4)	60(6)	5(4)	5(4)	-5(5)
C7	57(5)	61(5)	57(5)	-8(3)	-8(3)	-16(4)
C8	56(5)	63(4)	51(4)	6(4)	6(4)	-7(4)
C9	57(5)	42(4)	59(5)	-3(4)	-3(4)	0(4)
C10	46(5)	34(4)	43(5)	2(4)	2(4)	-8(4)

	U^{11}	U^{22}	U^{33}	U^{23}	U^{13}	U^{12}
C11	73(4)	31(4)	68(4)	1(3)	1(3)	2(3)
C12	105(5)	38(4)	80(5)	-14(4)	-14(4)	10(3)
C13	44(5)	40(4)	60(5)	-1(4)	-1(4)	-12(3)
C14	40(5)	31(4)	37(5)	-2(4)	-2(4)	-18(4)
C15	40(5)	28(4)	47(5)	-4(4)	-4(4)	-6(4)
C16	45(4)	38(4)	59(5)	-2(4)	-2(4)	3(4)
C17	42(5)	50(4)	61(5)	9(4)	9(4)	4(3)
C18	59(5)	49(4)	109(6)	15(5)	15(5)	6(4)
C19	65(4)	41(5)	97(6)	13(4)	13(4)	12(3)
C20	48(5)	35(4)	75(5)	7(4)	7(4)	1(3)
C21	61(5)	44(5)	59(5)	-4(4)	-4(4)	-8(4)
C22	81(6)	56(4)	73(5)	-1(4)	-1(4)	-2(5)
C23	100(7)	72(5)	95(6)	-5(5)	-5(5)	-8(5)
C24	66(5)	67(5)	107(6)	-13(5)	-13(5)	5(4)
C25	87(6)	64(5)	112(7)	-9(5)	-9(5)	-18(5)
C26	72(5)	45(5)	107(6)	3(4)	3(4)	-2(4)
C27	42(4)	35(4)	92(6)	-6(5)	-6(5)	-1(3)
C28	49(5)	24(4)	63(5)	8(4)	8(4)	-9(4)
C29	42(4)	29(4)	83(5)	4(4)	4(4)	0(4)
C30	45(5)	50(5)	131(7)	-10(5)	-10(5)	7(3)

	U^{11}	U^{22}	U^{33}	U^{23}	U^{13}	U^{12}
C31	55(5)	76(5)	91(5)	11(4)	11(4)	2(4)
C32	49(5)	77(5)	89(5)	39(5)	39(5)	22(4)
C33	41(5)	30(4)	64(5)	5(4)	5(4)	-6(4)
C34	48(5)	42(4)	80(5)	1(3)	1(3)	5(4)

Table 5. Hydrogen coordinates ($x10^4$) and isotropic displacement parameters ($Å^2x10^3$) for dibenzaspirocyclopentane.

	x	y	z	U(eq)
H1	8300	4961	4555	87
H2A	7814	2517	3488	66
H2B	8458	1663	4167	66
H5	7583	2806	1995	69
H6	7337	806	952	75
H7	8141	-1588	873	71
H8	11029	1077	4971	68
H9	9995	2990	4605	60
H11A	9469	5048	3176	67
H11B	8640	5273	2676	67

	x	y	z	U(eq)
H12	8904	7031	3932	85
H13	9186	-2093	1852	56
H16	10309	-2095	3100	55
H17	11176	-1465	4224	61
H18	6639	1943	-482	87
H19A	5720	3849	-1393	88
H19B	6404	3721	-1717	88
H22	5535	6028	-166	88
H23	4490	7748	-200	102
H24	4074	10142	-1090	94
H25	7273	8080	-3104	101
H26	6384	10371	-3496	92
H27	5564	10883	-2823	70
H30	7337	6183	-2059	94
H31A	7473	6845	-561	98
H31B	6938	7388	-75	98
H32	7406	4133	338	89
H34	4700	10839	-1952	72